Homogenization and polarization of the seasonal water discharge of global rivers in response to climatic and anthropogenic effects

Homogenization and polarization of the seasonal water discharge of global rivers in response to climatic and anthropogenic effects

Abstract: We investigate global trends in seasonal water discharge using data from 5668 hydrological stations in catchments whose total drainage area accounts for 2/3 of the Earth's total land area. Homogenization of water discharge, which occurs when the gap in water discharge between dry and flood seasons shrinks significantly, affects catchments occupying 2/5 of the total land area, and is mainly concentrated in Eurasia and North America. In contrast, polarization of water discharge associated with widening of the gap in water discharge between dry and flood seasons, occurs in catchments covering 1/6 of the land area, most notably in the Amazon Basin and river basins in West Africa. Considering the major climatic and anthropogenic controlling factors, i.e. precipitation (P), evaporation (E), glacial runoff (G), and dam operations (D), the world's river basins are classified as P, DEP, GEP, and EP types. Contributions from each controlling factor to either the homogenization or polarization of the seasonal water discharge for each type of river have been analyzed. We found that homogenization of discharge is dominated by dam operations in GDEP and DEP river basins (contributing 48% and 64%) and by homogenized precipitation in GEP and EP river basins. Evaporation and precipitation are primary factors behind the polarization of discharge, contributing 56% and 41.2%. This study provides a basis for a possible decision tool for controlling drought/flood disasters and for assessing and preventing ecological damage in endangered regions.

Keywords: dam operations; evaporation; glacial runoff; global trends; precipitation; seasonal runoff.

1. Introduction

The world's rivers carry 40% of precipitation as runoff from land, and 95% of sediment to oceans, linking together the atmosphere, hydrosphere, and biosphere (Walling, 2006; Gerten et al., 2008). Recent climate change and human activities have greatly altered seasonal flows in rivers, with considerable repercussions for the frequencies of flood and drought events (Meko et al., 2007; Piao et al., 2007; Hirabayashi et al., 2013; Best, 2019). There have also been distinct impacts on the ecological environment, as evidenced by reductions in freshwater fish stocks in the US and Brazil (Poff et al., 2007; Petesse & Petrere, 2012), and changes to thermal regimes of rivers supplied by glacial and snow melt waters (Castella et al., 2001; Isenko et al., 2005; Caissie, 2006; Hari et al., 2010; Van Vliet et al., 2013; Cardenas et al., 2014 Mellor et al., 2017). Furthermore, it has been assessed by the International Panel on Climate Change (IPCC) that flood and drought events will be more frequent and severe in the future (Ahn et al., 2018).

Accelerating climate change can alter river flow allocation during dry and flood seasons (Chai et al., 2019a; Chai et al., 2019b). Researchers have suggested that changing precipitation and evaporation patterns have led to flood seasons getting wetter (0.94 ± 0.20 mm d^{-1} per century), and dry seasons getting drier (-0.53 ± 0.10 mm d^{-1} per century) (Wentz et al., 2007; Chou & Lan, 2012; Chou et al., 2013; Asadieh & Krakauer, 2015; Murray-Tortarolo et al., 2016) (see Fig. 1a). In contrast, glaciers have melted earlier than before due to increased temperature. Consequently, stream flows have tended to increase in dry seasons and decrease in flood seasons (Fig. 1b), particularly in rivers sustained primarily through snow-melting (Barnett et al., 2005; Li et al., 2008; Huss, 2011; Gan et al., 2015).

Human disturbance also alters the seasonal water discharge of rivers (Zhang & Lu,

2009; Grafton et al., 2013). Dam construction is perhaps the most widely distributed form of human activity affecting rivers over the past decades. By 2010, the total number of the world's large dams (higher than 15 m) reached more than 50,000, with a total capacity of 7000–8300 km^3 (Lehner et al., 2011; Li et al., 2015; Tilt & Gerkey, 2016). In flood seasons, the river flow is usually stored in the dam reservoir to prevent or alleviate flooding downstream, whereas in dry seasons water is released to meet navigation, water supply, and electricity generation needs (Arheimer et al., 2017; Bormann et al., 2011). Taking for instance the largest hydraulic structure in China, the Three Gorges Dam, located in the Yangtze River, the water volume stored during the flood season in 2011 was up to 17×10^9 m^3, while that released during the dry season was up to 15×10^9 m^3 (Chai et al., 2019a). Increased regulation of water flow by dams has thus progressively narrowed the gap in stream flow between flood and dry seasons (Fig. 1c).

Under the widespread impacts of climatic and anthropogenic factors, variations in intra-year patterns of water discharge have become more complex at global scale. To date however, researchers have tended to focus on particular rivers (Dai et al., 2008; Kundzewicz et al., 2015; Ogden et al., 2013; Xu et al., 2010). A notable exception is the study by Poff et al. (2007) of the distribution of intra-year water discharge in rivers at large scale (i.e. across the south of the United States). Even so, a comprehensive understanding of the quantitative impacts of major climatic and anthropogenic factors on seasonal flow patterns in global rivers has yet to be fully developed.

In this paper, we attempt to reveal the global patterns of the intra-year distribution of water discharge observed at 5668 hydrological stations, which monitor discharges from catchments occupying 66.1% of the Earth's total land surface area. To reflect the impacts of major climatic and anthropogenic factors, such as premature glacial melting

(G), dam operations (D), evaporation (E), and precipitation (P), we classify global river basins into four categories: GDEP (under the impacts of G, D, E, P factors, similarly hereinafter), DEP, GEP, and EP river basins. Based on testable hypothesis (see Data and Methods), separate contributions of each factor to either homogenization or polarization of water discharge for each category of river basin are estimated and interpreted.

2. Data and Methods

2.1 Data sources

Time series of daily and monthly discharges at 5668 hydrological stations in 3550 rivers were obtained from the Global Runoff Data Centre (https://www.cuahsi.org/data-models/portals/global-runoff-data-centre). 937 of the considered rivers (26.4%) have at least 2 gauging stations on them. The collected river basins occupy about 66% of the Earth's land area (Fig. S1a). Each of the watershed areas of these global rivers is larger than 2118 km^2. Of the rivers considered, 44 and 19 were in the world's top 50 and 20 largest rivers. To determine a statistically acceptable variation trend in seasonal runoff, only long-term series of discharge data were used, commencing in 1861 and ending in 2018 (all years are calendar years). For the global distribution of hydrological stations, 74.2% (4205 stations), 45.1% (2555 stations), 23.6% (1339 stations), 12.5% (708 stations) provided data exceeding 20, 40, 60, and 80 years respectively. Sufficient data series were available in both space and time to reveal the hydrological regimes of seasonal runoff at global scale.

To assess the effect of disturbance from human activities on seasonal differences in

runoff, records concerning 4622 dams in the study area were extracted from the Global Reservoirs and Dams database (GRanD, http://globaldamwatch.org/grand/) (Fig. S1b&c). The cumulative storage capacity of these dams is up to 5422 km^3, covering about 65–77% of the world's total storage capacity of large dams.

To explore the relationship between climate variation trend and seasonal runoff, daily climatological data on precipitation, temperature, and potential evapotranspiration during the period from 1901 to 2017, were gathered from the Climatic Research Unit (CRU, http://www.cru.uea.ac.uk/). The dataset covers the Earth's land surface at a spatial resolution of $0.5^\circ \times 0.5^\circ$.

2.2 Classification of global rivers

Based on the geographical location of river dams, the Earth's land surface can be divided into watersheds with and without dam operations, accounting for 72.1% and 27.9% of the study area (Fig. 1d). Regions containing glaciers or where the percentage of snow precipitation exceeds 20% are commonly regarded as snow melt-dominated (Barnett et al., 2005). Similarly, the entire research area can also be divided into river basins with (46.7% of the total area) and without glacier-melting (53.3% of the total area) as shown in Fig. 1d. Using this approach the global rivers are categorized into GDEP, GEP, DEP and EP types (Fig. 1e).

2.3 Division of dry and flood seasons

To reveal the seasonal hydrological regimes, each calendar year is divided into two mutually exclusive dry and flood seasons. The flood season is taken to be the period

when the stream flow in rivers shows a periodically increasing trend (Lei et al., 2017). Based on this hypothesis, the six consecutive months with the highest sum of runoff are categorized as the flood season, the remaining six months constitute the dry season. For example, the dry season extends from June to November in the Amazon River Basin (Zemp et al., 2017); the flood season of the Yangtze River lasts from May to October (Gemmer et al., 2008).

2.4 Trend analysis of normalized seasonal water discharge, precipitation, evaporation and glacial runoff

To examine different allocation regimes of seasonal water discharge, precipitation, evaporation, and glacial runoff between dry and flood seasons, a normalization method was applied, converting the data series of the dry or flood season into dimensionless values through division by the total annual values (He et al., 2002). Hence, changes in normalized values between the two seasons in different years reflect the adjustment of seasonal characteristics with time. Similarly, the data series of precipitation, potential evaporation, and glacial runoff of the global watersheds were also normalized in order to explore the mechanisms behind the redistribution of seasonal runoff in more detail.

We applied an improved Mann-Kendall method, the Mann-Kendall trend test with trend-free pre-whitening (TFPW-MK) method, to analyze variation trends in normalized river flow, precipitation, potential evapotranspiration, and glacial runoff in dry seasons, under the hypothesis that the climatic series are stochastically independent (Su et al., 2018; Li et al., 2019).

142 *2.5 Calculation of precipitation, evaporation, temperature and glacial runoff for each*
143 *basin*

144 The Thiessen Polygon Method (Liu et al., 2012; Barbulescu, 2015; Su et al.,
145 2018) was used to calculate the spatially averaged daily precipitation, potential
146 evaporation, and temperature of each watershed during the period from 1901 to
147 2017.

148 Glacier-dominated river basins (Fig. S2) are defined as basins either with
149 glaciers or where the snow fraction in precipitation is larger than 20% (Arheimer et
150 al., 2017). We used the well-established Degree-Day Model that relates air
151 temperature to snow and glacier melt rate to estimate glacial runoff (Ohmura, 2001;
152 Hock, 2003; Zhang et al., 2012; Seguinot, 2013). Despite its simplicity, the Degree-
153 Day Model has proved very accurate at representing melt behavior, often
154 outperforming energy-balance models at catchment scale (US Army Corps of
155 Engineers, 1971; WMO, 1986; Zhang et al., 2006). The model equations for
156 calculating the daily glacial runoff are as follows:

157 $$M(i)=\begin{cases} DDF\cdot(T(i)-T_{\mathrm{T}}) & T(i)>T_{\mathrm{T}} \\ 0 & T(i)\le T_{\mathrm{T}}, \end{cases} \quad (1)$$

158 where $M(i)$ is the glacial runoff on the i-th day (mm); DDF is the degree-day factor
159 (mm.^{o}C^{-1}), which is basin-specific; $T(i)$ is the average air temperature in the i-th
160 day (^{o}C); and T_T is the critical temperature of melting (generally selected as 0 ^{o}C).
161 Thus, the normalized glacial runoff, which is determined as the percentage of glacial
162 runoff in flood or dry seasons, can be calculated as:

$$M_{\mathrm{N}}=\frac{M_{\mathrm{F/D}}}{M_{\mathrm{T}}}=\frac{\sum_{\text{Flood or Dry seasons}} M(i)}{\sum_{\text{Total year}} M(i)}=\frac{\sum_{\text{Flood or Dry seasons}} M(i)/DDF}{\sum_{\text{Total year}} M(i)/DDF} \quad (2)$$

where M_N is the normalized glacial runoff in flood or dry seasons; $M_{F/D}$ is the glacial runoff in flood or dry season; M_T and is the annual total glacial runoff. It should be noted from Eq. (1) that $M(i)/DDF$ only depends on $T(i)$ and T_{T}, which means M_{N} is also temperature-dependent, and so is sensitive to the accuracy of temperature observations. According to Akhtar et al. (2009), uncertainty of temperature data in this study is 0.5-1.3 ^{o}C, implying an error of 3.0-7.7% in the calculation of glacial runoff.

2.6 Assessing the Degree of Regulation (DOR)

It is commonly assumed that the larger the cumulative storage capacity of a dam, the greater is its impact on redistribution of seasonal runoff. We therefore selected the Degree of Regulation (DOR) index to reflect the potential impact of dam operations on downstream seasonal river flows (Arheimer et al., 2017; Lehner et al., 2011; Grill et al., 2014). The DOR index is equal to the cumulative dam storage capacity of a sub-region divided by the average annual runoff of this sub-region (Eq. 3).

$$\mathrm{DOR}=\frac{\sum_{1}^{n} v(i)}{R} \quad (3)$$

where n is the number of dams in the sub-region; $v(i)$ is the storage capacity of the i-th dam (km^3); and R is the average annual runoff of the sub-region (km^3).

2.7 Calculation of contributions of climatic and anthropogenic controls to the homogenization and polarization of water discharge

Under the hypothesis that the explaining variables are not linearly related with each other, stepwise regression was performed to assess the relative contributions by key factors to changes in seasonal water discharge. Stepwise regression is a method of fitting regression models that involves starting with only one variable in the model. By testing the addition of each new variable using a model fit criterion, only those variables whose inclusion produce the most statistically significant improvement of the fit, are included. The process is repeated until no other variable improves the model significantly. After the stepwise regression analysis, the standardized regression coefficients that represented the relative size of the effects of different variables (Kaufman, 1996; Kim, 2011) were then used to calculate the contributions of precipitation, evaporation, glacial runoff, and dam operations to the changed allocation of water discharge between dry and flood seasons for each river basin. The higher the value of standardized coefficient of a controlling factor, the more significant the factor's effect. Thus the contributions of changes in precipitation, evaporation, glacial runoff, and dam operation to the allocation changes of the seasonal runoff between dry and flood seasons, R_p, R_e, R_g and R_d, were calculated from:

$$R_p = \frac{b_p}{b_b + b_e + b_g + b_d} \quad (4)$$

$$R_e = \frac{b_e}{b_b + b_e + b_g + b_d} \quad (5)$$

$$R_g = \frac{b_g}{b_b + b_e + b_g + b_d} \quad (6)$$

$$R_d = \frac{b_d}{b_b + b_e + b_g + b_d} \quad (7)$$

where b_p, b_e, b_g and b_d are the standardized coefficients of precipitation, evaporation, glacial runoff, and dam operation.

3. Results

3.1 Distribution of GDEP, DEP, GEP, and EP river basins

The accumulated catchment areas of GDEP and DEP accounted for 38.6% and 33.5% of the study area (Fig. 1e), indicating that the majority of global river basins were affected by dam operations. By comparison, the areas of EP and GEP had very values of 1735.4×10^4 km^2 (19.7%) and 722.4×10^4 km^2 (8.2%), respectively. Among the world's top 20 rivers, most are GDEP rivers, but none is a GEP river (Table S1). It is interesting to note that all GDEP and GEP river basins are situated in the Northern Hemisphere, implying that the impact of glacial melting seldom extends to the Southern Hemisphere.

At continental scale, the GDEP river basins are widely distributed in Asia (1868.5×10^4 km^2), North America (1102.5×10^4 km^2), and Eastern Europe (376.7×10^4 km^2), whereas DEP and EP river basins are mainly located in Western Europe, South America, Africa and Oceania. By contrast, the GEP rivers are very near to the Arctic Circle (Fig. 1e).

3.2 Homogenization and polarization of intra-year discharges

Fig. S3 shows an obvious spatial heterogeneity in the division between dry and flood season periods at each station. In the Northern Hemisphere, the dry season mostly occurs from October to March (21.6%) and from November to April (31.4%), whereas the dry season in the Southern Hemisphere is taken to be primarily from May to October (15.8%) and from June to November (33.3%).

When the water discharges in dry and flood seasons were transformed into normalized values at each station, it is found that the normalized discharge in the dry season increased at 22.7% of the hydrological stations (1287 stations) with confidence level exceeding 90% (Fig. 2a, and see details in Figs. S4), remarkably narrowing the gap in water discharge between dry and flood seasons; we call this water discharge homogenization. Discharges from 26.2% of the stations in Northern Hemisphere and from 12.3% of the stations in the Southern Hemisphere have been homogenized. High percentages of stations with homogenized water discharge occur in North America (34.1%), Asia (24.9%), and Europe (18.8%), whereas low percentages with homogenized water discharge appear in South America (14.1%), Oceania (13.7%), and Africa 10.8%). An opposite trend occurred at 8.3% of the hydrological stations (470 stations), where the gap in water discharge increased between dry and flood seasons (which we call water discharge polarization). No obvious variation or trends were evident at the remaining hydrological stations. In contrast, discharges from 6.0% of the stations in Northern Hemisphere and from 15.3% of the stations in the Southern Hemisphere have been polarized. High percentages of stations with polarized water discharge occur in Oceania (17.6%), South America (15.3%), and Africa (14.8%), whereas low percentages with polarized water

discharge appear in Europe (8.1%), Asia (5.1%), and North America (4.7%).

To determine whether an independent basin (defined as one that is hydrologically independent and is not contained by any others considered in the study) has been experiencing water discharge homogenization or polarization, we select the intra-year water discharge observed at the hydrological station located at (or nearest to) the estuary as representative of the overall trend in the basin. From the resulting values, we find that water discharge homogenization has occurred in 181 of the 314 independent basins examined, occupying up to 62.6% (5513.4×10^4 km^2) of the total area studied, whereas water discharge polarization was experienced by 39 independent basins covering 25.6% of the total area studied (Fig. 2f). Noting that the lengths of water discharge series observed at the end hydrological stations of each basin are different, we can also analyze the temporal characteristics of water discharge homogenization or polarization. In the period preceding 1980, only 25.0% of the total study area experienced water discharge homogenization, being mainly scattered in North America and West Asia (Fig. 2b). However, considerable areas of East Asia, Europe, Africa, and South America began to experience water discharge homogenization by the end of the 1980s, with the area affected having spread to 51.9% of the total study area (Fig. 2c). Meanwhile, water discharge polarization gradually appeared in West Africa, South America, and Central Australia from the 1980s to 2000s (Figs. 2c, d and e).

It should be noted that homogenization of water discharge occurred in 13 of the top 20 world largest river basins, including the Nile, Mississippi, Ob, Paraná, Yenisei, Lena, Tamanrasett, Yangtze, Amur, Mackenzie, Ganges, Volga, and Zambezi. For example, the Mississippi River (Vicksburg station) experienced a 13.2% increase in multi-year average percentage of normalized discharge in dry seasons during 1960–

1989 in comparison to that in 1932–1959, and further rose by 17.4% during 1990–2017. However, only six of the top 20 world's largest river basins, the Amazon, Zaire, Niger, Lake Chad, Great Artesian, and Indus, exhibited polarization of water discharge. Taking the Snake River (Neeley station) as an example, the normalized discharge in the dry season reduced markedly over time, with average percentages during periods of 1951–1980 and 1981–2016 falling by 17.5% and 39.2% compared to 1908–1950. As the longest river basin in the world, the Nile, a typical DEP river basin, began to exhibit water discharge homogenization during the 1980s. Certain major glacier-sourced river basins, classified as GDEP type, such as in the Yenisei, Lena, and Amur River basins in Russia, began to exhibit water discharge homogenization in the 1980s when a global warming trend started to be more evident (Hu et al., 2019). Also belonging to the GDEP type, the Yangtze River basin, which contains the largest number of dams of any basin in the world, started to show a water discharge homogenization trend during the 1990s. At about the same time, polarization of water discharge started to occur in the Amazon River basin, an EP basin carrying the largest discharge in the world. In the 2000s, the water discharge polarization began to prevail in the Zaire River basin, a more typical representative of an EP basin.

3.3 Co-varying trends in the natural factors and water discharge

Natural factors which may influence the intra-year distribution of water discharge, such as precipitation, evaporation, and glacial runoff, are also experiencing homogenization or polarization trends in certain areas of the world. Fig. 3a shows that the gap in precipitation between dry and flood seasons significantly narrowed in 20.4% of the study area and widened in 10.5% of the study area. As shown in Fig. S5 and Table S2, areas with homogenized precipitation in Asia, North

America, Africa, Europe, South America, and Oceania accounted for 9.5%, 6.3%, 2.5%, 1.3%, 0.2%, and 0.0% of the study area respectively, while those with polarized precipitation only covered 1.3%, 1.3%, 0.0%, 0.03%, 7.3%, and 0.0% of the study area in the above continents. Among the world's top 20 largest rivers, the gap in seasonal precipitation between dry and flood seasons narrowed significantly in the Nile, Ob, Yenisei, and Amur River basins, while that in the Amazon and Tamanrasett river basins grew. We also found in the inset histogram of Fig. 3a that 16.4–32.6% and 14.3–44.6% of the drainage areas characterized by homogenization and polarization of seasonal water discharge, respectively, also experienced identical trends in seasonal precipitation, implying that precipitation might be a primary factor influencing the intra-year distribution of water discharge in these regions.

Figure. 3b shows that the gap in seasonal evaporation between dry and flood seasons became enlarged in the 17.6% of the study area, but shrank in 70 basins (12.9% of the study area). As displayed in Fig. S6 and Table S3, areas with homogenized evaporation were most widely distributed in Africa, Asia, and North America, covering 7.0%, 5.8%, and 2.3% of the study area, and merely 1.2%, 0.2%, and 0.1% of the study area in South America, Oceania, and Europe. Most regions with polarized evaporation were scattered in North America, Europe, and Asia, representing 7.4%, 2.0%, and 1.4% of the study area, whereas only 0.9%, 0.0%, and 0.0% of the study area experienced polarized trends in evaporation in South America, Oceania, and Africa. Among the world's top 20 largest river basins, the Zaire, Ob, Niger, and Amur all exhibited significant polarization trends in normalized

evaporation with a confidence level > 95%, whereas normalized evaporation in the Mississippi and Mackenzie River basins was obviously homogenized. Noting that the direction of water transfer during evaporation is opposite to that during precipitation, variations in evaporation lead to opposite effects on the seasonal river discharge compared with the impacts of precipitation. In other words, polarized evaporation and homogenized precipitation contribute to the homogenization of water discharge, and conversely homogenized evaporation and polarized precipitation lead to polarization of water discharge. The inset histogram of Fig. 3b summarizes the co-varying trends in polarized evaporation and homogenized water discharge, as well as the co-varying trends in homogenized evaporation and polarized water discharge. It indicates that 17.1% and 28.9% of the total area characterized by homogenization and polarization of water discharge experienced opposite trends in seasonal evaporation.

We applied a degree-day model to estimate the glacial runoff in basins supplied mainly by glacial or snow melt water, and found that the difference in allocation of glacial runoff between dry and flood seasons narrowed in most drainage areas (Fig. 3c, and see details in Fig. S7 and Table S4), covering 5.6% of the total study area (494.9×10^4 km^2). Most of these river basins (463.9×10^4 km^2) also experienced homogenization of water discharge. It can also be inferred from the inset histogram in Fig 3c that the impact of premature glacial melting on the homogenization of water discharge became increasingly obvious as time progressed. By contrast, the gap in glacial runoff between the dry and flood seasons grew in only 8 river basins (an example being the Mississippi River basin) whose area occupied about 4.2% (371.2

341 km^2) of the total study area. However, none of these basins exhibited polarization in
342 water discharge.

343 *3.4 Co-distribution of dam construction and intra-year water discharge trends*

344 In terms of human interference to global rivers, reservoir operations have
345 perhaps the largest impact. In recent years, many very large dams have been
346 constructed along major rivers to meet human needs for energy, flood prevention,
347 shipping, irrigation, and recreation. Here we adopt the degree of regulation (DOR),
348 defined as the ratio of the cumulative storage capacity to annual runoff, to further
349 investigate the impact of dams on seasonal homogenization of water discharge. A
350 high value of DOR implies that dam operations are having a significant effect on the
351 hydrological regime. Fig. 3d indicates that 195 of the 314 basins have been
352 significantly regulated by dams (i.e. where DOR $\geq$ 2%) (Nilsson et al., 2005). For 95
353 basins, DOR exceeds 50%, and their overall area accounts for 37.5% of the total
354 study area. At continental scale, Asia, North America, and Europe experienced the
355 greatest, second greatest, and third greatest effects of dam operations on river flow
356 with 16.2%, 5.1%, and 3.2% of the study area having a DOR that was larger than 2%
357 respectively. By contrast, only 2.8%, 2.3%, and 0.1% of the study area located in
358 Africa, South America, and Oceania had high DOR (> 2%) (see details in Fig. S8 and
359 Table S5). The inset histogram in Fig. 3d shows that 91.0% of the drainage area
360 exhibiting homogenization in water discharge also experienced radical dam
361 construction, implying that the homogenization in water discharge might be closely
362 associated to the operation of dams.

3.5 Contributions of major factors to homogenization and polarization of seasonal water discharge

Using the stepwise regression method, we found that the operation of dams was the dominant factor behind the global homogenization of seasonal water discharge in all the 181 river basins (contributing 41.9%), with homogenized precipitation, polarized evaporation, and premature glacial melting, contributing 28.0%, 21.4%, and 8.7%, respectively. In GDEP and DEP river basins, dam operations remain the major reason for the homogenization of seasonal water discharge (contributing 52–64% and 30–57%), followed by polarized evaporation (contributing 13–22% for GDEP rivers and 22–33% for DEP rivers), homogenized precipitation (contributing 13–18% and 19–48% for GDEP and DEP rivers), and premature glacial melting (contributing 7–17% in GDEP rivers) (Table 1). For example, the Yangtze river, a GDEP river that contains the world's largest dams, has been seriously affected by dam operations, with the associated contribution to the water discharge homogenization reaching 80.8%. It should be noted that, although the Nile River basin is intensively regulated (DOR reaching 431%), the contribution of dam operations to water discharge homogenization is rather small. This is because the Aswan High Dam located on the Nile River engages a multi-year regulating scheme (El-Shafie et al., 2007). Therefore, dam operations lead to the redistribution of water discharge at the multi-year scale rather than the intra-year scale. Homogenized precipitation and polarized evaporation are found to be the primary factors behind the homogenization in water discharge of the Nile River basin, contributing 68.0% and 32.0%, respectively. For GEP river basins (Table 1), the major driving factors were premature glacial melting during the period before 1980 (85%), altering to polarized evaporation during 1980–2010 (48–69%), and changes in homogenized

precipitation in the 2010s (38%). For EP rivers (Table 1), the impact of precipitation variation on water discharge homogenization grew, with its contribution increasing from 24% in the period before 1980 to 93% by the 2010s, while the effect of variation in evaporation declined.

Among the 39 river basins (25.6% of the total study area) affected by polarization of seasonal water discharge, EP river basins occupied the largest drainage area (1495.8×10^4 km^2 accounting for 66.2% of the total area characterized by polarized discharge), with GDEP, DEP, and GEP river basins taking up only 11.4%, 18.6%, and 3.8%. Homogenized evaporation and polarized precipitation were the major causal factors behind the global water discharge polarization in the 39 basins, contributing 56.0% and 41.2%, whereas polarized glacial runoff merely contributed 2.8%, and dam operations had no impact. The importance of polarized precipitation has grown with time for the GDEP, DEP and GEP river basins (Table 1). In contrast, EP river basins with water discharge polarization are increasingly affected by homogenized evaporation (Table 1). As a typical EP river, evaporation accounts for 87.3% of water discharge polarization for the Amazon Basin, which is not surprising given that evapotranspiration contributes 48 – 80% of local rainfall in this enormous basin (Salati et al., 1979; Martinelli, et al., 1996; Marengo, 2005). Detailed contributions of each factor at basin-level are given in Fig. S9, and at continental-level in Table S6.

4. Discussion

Although taking up a relatively small percentage of the global land area, river basins with polarized water discharges may have a profound effect on human welfare, by contributing more frequent floods or droughts, especially when the total annual

discharge changes. According to Li et al. (2019), 24% of the world's large rivers have experienced significant changes in total annual water fluxes. Among those river basins, the risk of droughts will continue to increase in the Haihe River in China, and the Niger, Senegal, and Limpopo rivers in Africa, where the decrease in total annual water fluxes coincides with the polarization of intra-year discharges. By contrast, the likelihood of floods will increase in rivers with polarized discharges located around the Arctic Circle, where total discharges mostly exhibit an increasing trend. The likelihoods of both drought and flood events will increase in rivers with polarized intra-year discharge and stable total annual discharge, such as the Amazon and the Indus. Noting that changes in total water fluxes are highly dependent on variations in climatic controlling factors (Li et al., 2019), which, *inter alia*, are also the primary reasons behind polarization of the intra-year discharges. This implies that the characteristics of climate change generally control the occurrence of extreme discharge events in rivers. The Fifth Assessment Report by IPCC (2014) suggested that precipitation will increase around the Arctic Circle and in central Africa by 2100, enhancing flood risk in the Niger and GEP river basins. However, the climate will become progressively drier in the northern part of South America in the next 100 years, elevating the likelihood of droughts in the Amazon River basin. It should also be noted that polarization of water discharge is more prevalent in the Southern Hemisphere, raising the risks of more frequent drought and flooding events above those in the Northern Hemisphere.

Homogenization of water discharge often correlates with damage of ecological systems in aquatic environments, most notably in rivers under direct impact of glacial melting, where the thermal regime often changes as glacial runoff redistributes (Castella et al., 2001; Caissie, 2006; Hari et al., 2010). Therefore, special attention

should be given to populations of aquatic organisms sensitive to thermal conditions in GEP rivers in and around the Arctic Circle, where premature glacial melting contributes up to 30% to the homogenization of water discharge. For the homogenization of water discharge dominated by dam operations, ecological problems related to the seasonal hydrodynamic conditions of rivers are most common. For instance, as a typical GDEP river basin, the Yangtze is one of the most intensively regulated in the world. With the contribution of dam operations to the homogenized water discharge reaching over 80%, the spawning grounds for some anadromous fish in the Yangtze River were severely affected by the variation in hydrodynamic conditions (Jiao et al., 2019). Note also that homogenization of water discharge mainly occurs in the Northern Hemisphere, where conservation strategies are urgently required to maintain ecosystem diversity.

5. Conclusions

By examining trends in normalized water discharges at 5668 hydrological stations, we found that seasonal water discharge homogenization and polarization occurred in basins occupying about 40% and 17% of the World's total land area. Dam operations made a major contribution (41.9%) to the homogenization of seasonal water discharge, followed by polarized evaporation, homogenized precipitation and premature glacial melting. Homogenized evaporation and polarized precipitation generally dominated the polarization of water discharge, contributing 56.0% and 41.2% respectively. Premature glacial runoff also had a significant effect on the seasonal water discharge homogenization and polarization, especially in GEP river basins, with contributions of 30% and 21% respectively. This study could provide a basis for a decision tool aimed at controlling drought/flood disasters, and a

methodology for assessing and preventing ecological damage in endangered regions.

Acknowledgements

This work was supported by the Youth Project of National Natural Science Foundation of China [grant number 41601275] and the National Key R&D Program of China [grant number: 2016YFA0600901]. AJD acknowledges support from the Netherlands Earth System Science Centre.

Data availability

Links to the data sets that support the findings of this study are available in the text.

References

Ahn, J. M., Kwon, H. G., Yang, D. S., Kim, Y. S. (2018). Assessing environmental flows of coordinated operation of dams and weirs in the Geum River Basin under climate change scenarios. Science of the Total Environment, 643, 912-925. https://doi.org/10.1016/j.scitotenv.2018.06.225

Akhtar, M., Ahmad, N.,Booij, M. J. (2009). Use of regional climate model simulations as input for hydrological models for the Hindukush-Karakorum-Himalaya region. Hydrol. Earth Syst. Sci, 13, 1075–1089. https://doi.org/10.5194/hess-13-1075-2009

Arheimer, B., Donnelly, C., & Lindstrom, G. (2017). Regulation of snow-fed rivers affects flow regimes more than climate change. Nature Communications, 8, 62. https://doi.org/10.1038/s41467-017-00092-8

Asadieh, B., & Krakauer, N. Y. (2015). Global trends in extreme precipitation: climate models versus observations. Hydrology and Earth System Sciences, 19, 877–891.

https://doi.org/10.5194/hess-19-877-2015

Barbulescu, A. (2015). A new method for estimation the regional precipitation. Water Resources Management, 30, 33-42. https://doi.org/10.1007/s11269-015-1152-2

Barnett, T. P., Adam, J. C., & Lettenmaier, D. P. (2005). Potential impacts of a warming climate on water availability in snow-dominated regions. Nature, 438, 303–309. https://doi.org/10.1038/nature04141

Best, J. (2019). Anthropogenic stresses on the world's big rivers. Nature Geoscience, 12, 7–21. https://doi.org/10.1038/s41561-018-0262-x

Bormann, H., Pinter, N., & Elfert, S. (2011). Hydrological signatures of flood trends on German rivers: flood frequencies, flood heights and specific stages. Journal of Hydrology, 404, 50–66. https://doi.org/10.1016/j.jhydrol.2011.04.019

Caissie, D. (2006). The thermal regime of rivers: a review. Freshwater Biology, 51, 1389–1406. https://doi.org/10.1111/j.1365-2427.2006.01597.x

Cardenas, M. B., Doering, M., Rivas, D. S., Galdeano, C., Neilson, B. T., & Robinson, C. T. (2014). Analysis of the temperature dynamics of a proglacial river using time-lapse thermal imaging and energy balance modeling. Journal of Hydrology, 519, 1963–1973. https://doi.org/10.1016/j.jhydrol.2014.09.079

Castella, E., Hákon Adalsteinsson, Brittain, J. E., Gislason, G. M., Lehmann, A., Lencioni, V. et al. (2001). Macrobenthic invertebrate richness and composition along a latitudinal gradient of european glacier-fed streams. Freshwater Biology, 46, 1811–1831. https://doi.org/10.1046/j.1365-2427.2001.00860.x

Chai, Y., Li, Y., Yang, Y. et al. (2019a) Water level variation characteristics under the impacts of extreme drought and the operation of the Three Gorges Dam. Frontiers of Earth Science, 13, 510–512. https://doi.org/10.1007/s11707-018-0739-3

Chai, Y. F., Li, Y. T., Yang, Y. P., Zhu, B. Y., Li, S. X., Xu, C., & Liu, C. C. (2019b).

513 Influence of climate variability and reservoir operation on streamflow in the
514 Yangtze River. Scientific Reports, 9, 5060. https://doi.org/10.1038/s41598-019-
515 41583-6
516 Chou, C., & Lan, C. W. (2012). Changes in the annual range of precipitation under
517 global warming. Journal of Climate, 25, 222–235. https://doi.org/10.1175/JCLI-D-
518 11-00097.1
519 Chou, C., Chiang, J. C. H., Lan, C. W., Chung, C. H., Liao, Y. C., & Lee, C. J. (2013).
520 Increase in the range between wet and dry season precipitation. Nature Geoscience,
521 6, 263–267. https://doi.org/10.1038/NGEO1744
522 Dai, Z. J., Du, J. Z., Li, J. F., Li, W. H., & Chen, J. Y. (2008). Runoff characteristics of
523 the Changjiang River during 2006: effect of extreme drought and the impounding
524 of the Three Gorges Dam. Geophysical Research Letters, 35, 521–539.
525 https://doi.org/10.1029/2008gl033456
526 El-Shafie, A., Taha, M. R., & Noureldin, A. (2007). A neuro-fuzzy model for inflow
527 forecasting of the Nile River at Aswan high dam. Water Resources Management,
528 21, 533–556. https://doi.org/10.1007/s11269-006-9027-1
529 Gan, R., Luo, Y., Zuo, Q., & Sun, L. (2015). Effects of projected climate change on the
530 glacier and runoff generation in the Naryn River Basin, Central Asia. Journal of
531 Hydrology, 523, 240–251. https://doi.org/10.1016/j.jhydrol.2015.01.057
532 Gemmer, M., Jiang, T., Su, B. D., & Kundzewicz, Z. W. (2008). Seasonal precipitation
533 changes in the wet season and their influence on flood/drought hazards in the
534 Yangtze River Basin, China. Quaternary International, 186, 12–21.
535 https://doi.org/10.1016/j.quaint.2007.10.001
536 Gerten, D., Rost, S., Von Bloh, W., & Lucht, W. (2008). Causes of change in 20th
537 century global river discharge. Geophysical Research Letters, 35, L20405.

https://doi.org/10.1029/2008GL035258

Grafton, R. Q., Pittock, J., Davis, R., Williams, J., Fu, G. B., Warburton, M. et al. (2013). Global insights into water resources, climate change and governance. Nature Climate Change, 3, 315–321. https://doi.org/10.1038/NCLIMATE1746

Grill, G., Ouellet Dallaire, C., Fluet Chouinard, E., Sindorf, N., & Lehner, B. (2014). Development of new indicators to evaluate river fragmentation and flow regulation at large scales: A case study for the Mekong River Basin. Ecological Indicators, 45, 148-159. https://doi.org/10.1016/j.ecolind.2014.03.026

Hari, R. E., Livingstone, D. M., Siber, R., Burkhardt□Holm, P., & Güttinger, H. (2010). Consequences of climatic change for water temperature and brown trout populations in alpine rivers and streams. Global Change Biology, 12, 10–26. https://doi.org/10.1111/j.1365-2486.2005.001051.x

He, Y. H., You, Q. Y., Zhong, H. M., & Yan, J. N. (2002). Study and application of the formation damage of potential sensitivity fast predicting software in Daqing oil field. Drill Fluid Compl Fluid, 19, 32-35. https://doi.org/10.3969/j.issn.1001-5620.2002.01.011

Hirabayashi, Y., Mahendran, R., Koirala, S., Konoshima, L., Yamazaki, D., Watanabe, S. et al. (2013). Global flood risk under climate change. Nature Climate Change, 3, 816–821. https://doi.org/10.1038/NCLIMATE1911

Hock, R. (2003). Temperature index melt modelling in mountain areas. Journal of Hydrology, 282, 104-115. https://doi.org/10.1016/S0022-1694(03)00257-9

Hu, X., Sejas, S. A., Ming, C., Taylor, P. C., Yi, D., & Song, Y. (2019). Decadal evolution of the surface energy budget during the fast warming and global warming hiatus periods in the ERA-interim. Climate Dynamics, 52, 2005–2016. https://doi.org/10.1007/s00382-018-4232-1

563 Huss, M. (2011). Present and future contribution of glacier storage change to runoff
564 from macroscale drainage basins in Europe. Water Resources Research, 47,
565 W07511. https://doi.org/10.1029/2010WR010299
566 IPCC. (2014). AR5 Synthesis Report - Climate Change 2014. Cambridge, UK:
567 Cambridge University Press.
568 Isenko, E., Naruse, R., & Mavlyudov, B. (2005). Water temperature in englacial and
569 supraglacial channels: change along the flow and contribution to ice melting on the
570 channel wall. Cold Regions Science and Technology, 42, 53–62.
571 https://doi.org/10.1016/j.coldregions.2004.12.003
572 Jiao, W. J., Zhang, P., Chang, J. B., Tao, J. P., Liao, X. L., & Zhu, B. (2019). Variation
573 in the suitability of Chinese sturgeon spawning habitat after construction of dams
574 on the Yangtze River. Journal of Applied Ichthyology, 35, 637–643. https://doi.org/
575 10.1111/jai.13914
576 Kaufman, R. L. (1996). Comparing effects in dichotomous logistic regression: a variety
577 of standardized coefficients. Social Science Quarterly, 77(1), 90-109.
578 https://doi.org/10.1177/053901896035001010
579 Kim, R. S. (2011). Standardized regression coefficients as indices of effect sizes in
580 meta-analysis [Doctoral dissertation]. United States of America: Florida State
581 University.
582 Kundzewicz, Z. W., Merz, B., Vorogushyn, S., Hartmann, H., Duethmann, D.,
583 Wortmann, M. et al. (2015). Analysis of changes in climate and river discharge
584 with focus on seasonal runoff predictability in the Aksu River
585 Basin. Environmental Earth Sciences, 73, 501–516.
586 https://doi.org/10.1007/s12665-014-3137-5
587 Lehner, B., Liermann, C. R., Revenga, C., Vorosmarty, C., Fekete, B. et al. (2011).

588 High-resolution mapping of the world's reservoirs and dams for sustainable river-
589 flow management. Frontiers in Ecology and the Environment, 9, 494–502.
590 https://doi.org/10.1890/100125
591 Lei, X., Xie, P., & Gu, H. T. (2017). A hydrological staging method based on variation
592 analysis of monthly runoff reconstruction sequence. Journal of Basic Science and
593 Engineering, 25, 211-220. https://doi.org/10.16058/j.issn.1005-0930.2017.02.001
594 Li, G., Wang, X. T., Yang, Z., Mao, C., West, A. J., & Ji, J. (2015). Dam-triggered
595 organic carbon sequestration makes the Changjiang (Yangtze) River Basin (China)
596 a significant carbon sink. Journal of Geophysical Research-Biogeosciences, 120,
597 39–53. https://doi.org/10.1002/2014JG002646
598 Li, L., Hao, Z. C., Wang, J. H., Wang, Z. H., & Yu, Z. B. (2008). Impact of future climate
599 change on runoff in the head region of the Yellow River. Journal of Hydrologic
600 Engineering, 13, 347–354. https://doi.org/10.1061/(ASCE)1084-
601 0699(2008)13:5(347)
602 Li, L., Ni, J. R., Chang, F., Yue, Y., Frolova, N., Magritsky D., et al. (2019). Global
603 trends in water and sediment fluxes of the world's large rivers. Science Bulletin.
604 https://doi.org/10.1016/j.scib.2019.09.012
605 Liu, J. Z., Zhu, A. X., & Duan, Z. (2012). Evaluation of TRMM 3B42 precipitation
606 product using rain gauge data in Meichuan Watershed, Poyang Lake Basin, China.
607 Journal of Resources and Ecology, 3, 359-366.https://doi.org/10.5814/j.issn.1674-
608 764x.2012.04.009
609 Marengo, J. A. (2005). Characteristics and spatio-temporal variability of the Amazon
610 River Basin water budget. Climate Dynamics, 24, 11–22.
611 https://doi.org/10.1007/s00382-004-0461-6
612 Martinelli, L. A., Victoria, R. L., Sternberg, L. S. L., Ribeiro, A., & Moreira, M. Z.

(1996). Using stable isotopes to determine sources of evaporated water to the atmosphere in the Amazon Basin. Journal of Hydrology, 183, 191–204. https://doi.org/10.1016/0022-1694(95)02974-5

Meko, D. M., Woodhouse, C. A., Baisan, C. A., Knight, T., Lukas, J. J., Hughes, M. K. & Salzer, M. W. Medieval drought in the Upper Colorado River Basin. Geophysical Research Letters, 34, 473–476 (2007). https://doi.org/10.1029/2007GL029988

Mellor, C. J., Dugdale, S. J., Garner, G., Milner, A. M., & Hannah, D. M. (2017). Controls on Arctic glacier-fed river water temperature. Hydrological Sciences Journal-Journal des Sciences Hydrologiques, 62, 499–514. https://doi.org/10.1080/02626667.2016.1261295

Murray-Tortarolo, G., Friedlingstein, P., Sitch, S., Seneviratne, S. I., Fletcher, I., Mueller, B. et al. (2016). The dry season intensity as a key driver of NPP trends. Geophysical Research Letters, 43, 2632–2639. https://doi.org/10.1002/2016GL068240

Nilsson, C., Reidy, C. A., Dynesius, M., & Revenga, C. (2005). Fragmentation and flow regulation of the world's large river systems. Science, 308, 405–408. https://doi.org/10.1126/science.1107887

Ogden, F. L., Crouch, T. D., Stallard, R. F., & Hall, J. S. (2013). Effect of land cover and use on dry season river runoff, runoff efficiency, and peak storm runoff in the seasonal tropics of Central Panama. Water Resources Research, 49, 8443–8462. https://doi.org/10.1002/2013WR013956

Ohmura A. (2001). Physical basis for the temperature-based melt-index method. Journal of Applied Meteorology, 40, 753-761. https://doi.org/10.1175/1520-0450(2001)040<0753:PBFTTB>2.0.CO;2

Petesse, M. L., & Petrere, M. (2012). Tendency towards homogenization in fish

assemblages in the cascade reservoir system of the Tietê River Basin, Brazil. Ecological Engineering, 48, 109–116. https://doi.org/10.1016/j.ecoleng.2011.06.033

Piao, S., Friedlingstein, P., Ciais, P., De Noblet-Ducoudre, N., Labat, D., & Zaehle, S. (2007). Changes in climate and land use have a larger direct impact than rising co2 on global river runoff trends. Proceedings of the National Academy of Sciences of the United States of America, 104, 15242–15247. https://doi.org/10.1073/pnas.0707213104

Poff, N. L., Olden, J. D., Merritt, D. M., & Pepin, D. M. (2007). Homogenization of regional river dynamics by dams and global biodiversity implications. Proceedings of the National Academy of Sciences of the United States of America, 104, 5732–5737. https://doi.org/10.1073/pnas.0609812104

Salati, E., Dall"Olio, A., Matsui, E., & Gat, J. R. (1979). Recycling of water in the Amazon Basin: an isotopic study. Water Resources Research, 15, 1250–1258. https://doi.org/10.1029/wr015i005p01250

Seguinot, J. (2013). Spatial and seasonal effects of temperature variability in a positive degree-day glacier surface mass-balance model. Journal of Glaciology, 59, 1202-1204. https://doi.org/10.3189/2013J0G13J081

Su, L., Miao, C. Y., Kong, D. X., Duan, Q. Y., Lei, X. H., Hou, Q. Q., & Li, H. (2018). Long-term trends in global river flow and the causal relationships between river flow and ocean signals. Journal of Hydrology, 563, 818-833. https://doi.org/10.1016/j.jhydrol.2018.06.058

Tilt, B., & Gerkey, D. (2016). Dams and population displacement on China's upper Mekong River: implications for social capital and social–ecological resilience. Global Environmental Change-Human and Policy Dimensions, 36,

153–162. https://doi.org/10.1016/j.gloenvcha.2015.11.008

US Army Corps of Engineers. (1971). Runoff evaluation and streamflow simulation by computer. (Part II). Portland, OR: North Pacific Division.

Van Vliet, M. T. H., Franssen, W. H. P., Yearsley, J. R., Ludwig, F., Haddeland, I., Lettenmaier, D. P. & Kabat, P. (2013). Global river discharge and water temperature under climate change. Global Environmental Change-Human and Policy Dimensions, 23, 450–464. https://doi.org/10.1016/j.gloenvcha.2012.11.002

Walling, D. E. (2006). Human impact on land–ocean sediment transfer by the worlds rivers. Geomorphology, 79, 192–216. https://doi.org/10.1016/j.geomorph.2006.06.019

Wentz, F. J., Ricciardulli, L., Hilburn, K., & Mears, C. (2007). How much more rain will global warming bring?. Science, 317, 233–235. https://doi.org/10.1126/science.1140746

World Meteorological Organization (WMO). (1986). Inter-comparison of snowmelt-runoff models. Geneva: World Meteorological Organization. (WMO Hydrological Report 23)

Xu, C. C., Chen, Y. N., Hamid, Y., Tashpolat, T., Chen, Y. P., Ge, H. T., & Li, W. H. (2010). Long-term change of seasonal snow cover and its effects on river runoff in the Tarim River Basin, Northwestern China. Hydrological Processes, 23, 2045–2055. https://doi.org/10.1002/hyp.7334

Zemp, D. C., Schleussner, C. F., Barbosa, H. M. J., Hirota, M., Montade, V., & Sampaio, G., et al. (2017). Self-amplified Amazon forest loss due to vegetation-atmosphere feedbacks. Nature Communications, 8, 14681. https://doi.org/10.1038/ncomms14681

Zhang, Q. S., Gao, X., Ye, B. S., Zhang, X. W., & Hagemann, S. (2012). A modified

monthly degree-day model for evaluating glacier runoff changes in China. Part II: application. Hydrological Processes, 26, 1697-1706. https://doi.org/10.1002/hyp.8291

Zhang, S., & Lu, X. X. (2009). Hydrological responses to precipitation variation and diverse human activities in a mountainous tributary of the lower Xijiang, China. Catena, 77, 130–142. https://doi.org/10.1016/j.catena.2008.09.001

Zhang, Y., Liu, S. Y., Xie, C. W., & Ding, Y. J. (2006). Application of a degree-day model for the determination of contributions to glacier meltwater and runoff near Keqicar Baqi glacier, Southwestern Tien Shan. Aannals of Glaciology, 43, 280-284. https://doi.org/10.3189/172756406781812320

699 **Figure Captions**

700

701 **Fig. 1.** Schematic illustration of changes in seasonal water discharge caused by
702 variations in evaporation and precipitation (a), premature glacial melting (b), and
703 reservoir operation (c). Panels (d) and (e) present four classifications of global rivers,
704 where E stands for evaporation, P for precipitation, D for dam operations, and G for
705 premature glacial melting impacts.

706

707 **Fig. 2.** Spatial-temporal variation characteristics of the water discharge
708 homogenization (HP, in blue) and polarization (PP, in red) for 314 independent river
709 basins covering 66.1% of the Earth's land surface (8809.2×10^4 km^2). Panel (a)
710 displays the variation trend in normalized water discharge at 5668 hydrological stations
711 during the dry season (checked using TFPM-MK trend test method). The remaining
712 panels comprise distribution maps of HP and PP based on data series extending to
713 the period before 1980 (b), by the 1980s (c), by the 1990s (d), by the 2000s (e) and
714 by the 2010s (f). Inset pie charts in (a), (b), (c), (d), (e) and (f) present the areal
715 percentages of HP (in blue), PP (in red), and no phenomenon (in yellow) in the five
716 periods.

717

718 **Fig. 3.** Panels (a), (b) and (c) are distribution maps showing the homogenized and
719 polarized precipitation, evaporation, and glacial runoff (represented by the blue and
720 red patches on the world map, respectively). Panel (d) maps the degree of regulation
721 (DOR) index observed in the last year of the water discharge series record for each
722 basin. The histogram insets in (a) and (c) present percentages of drainage areas
723 showing identical trends in precipitation and glacial runoff to the trends in seasonal

water discharge during the five periods of interest (Period 1: before 1980; Period 2: by 1980s; Period 3: by 1990s; Period 4: by 2000s; Period 5: by 2010s); the histogram inset in (b) presents percentages of drainage areas showing opposite trends in evaporation to the trends in seasonal water discharge during the five periods; the histogram inset in (d) presents percentages of drainage areas experiencing both homogenization water discharge and significant regulation by dams (DOR >2%) during the five periods; the blue bars represent regions with homogenization in water discharge; the red bars represent areas with polarization in water discharge.

732 **Table 1** Contributions of varied precipitation, evaporation, glacial runoff, and dam operations to water
733 discharge homogenization and polarization for four types of rivers during different periods.
734

River Type	Contribution (%)									
	Homogenization					Polarization				
	Before 1980s	By 1980s	By 1990s	By 2000s	By 2010s	Before 1980s	By 1980s	By 1990s	By 2000s	By 2010s
G	17	13	11	12	7	21	42	-	-	-
D	54	52	54	53	64	-	-	-	-	-
E	14	21	22	17	13	31	56	76	77	13
P	15	13	14	18	17	48	2	24	23	87
D	57	30	49	32	48	-	-	-	-	-
E	22	23	25	30	33	72	73	80	64	28
P	22	48	26	37	19	28	27	20	36	72
G	85	13	23	21	30	16	2	-	15	21
E	13	69	48	52	32	51	46	37	15	-
P	2	18	29	27	38	32	51	63	70	79
E	76	70	42	62	7	39	8	84	67	100
P	24	30	58	38	93	61	92	16	33	-

735

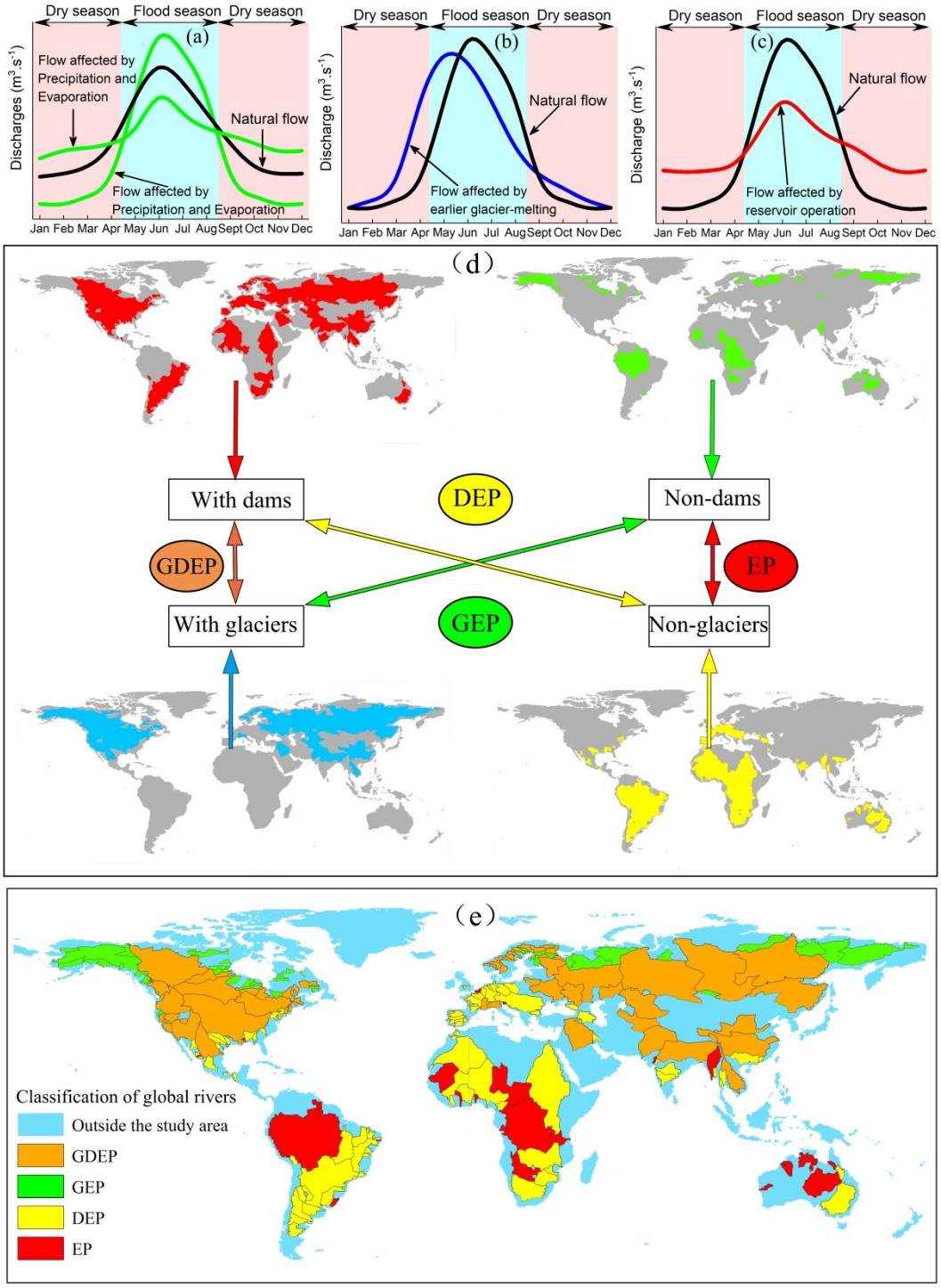

Fig. 1. Schematic illustration of changes in seasonal water discharge caused by variations in evaporation and precipitation (a), premature glacial melting (b), and reservoir operation (c). Panels (d) and (e) present four classifications of global river basins, where E stands for evaporation, P for precipitation, D for dam operations, and G for premature glacial melting impacts.

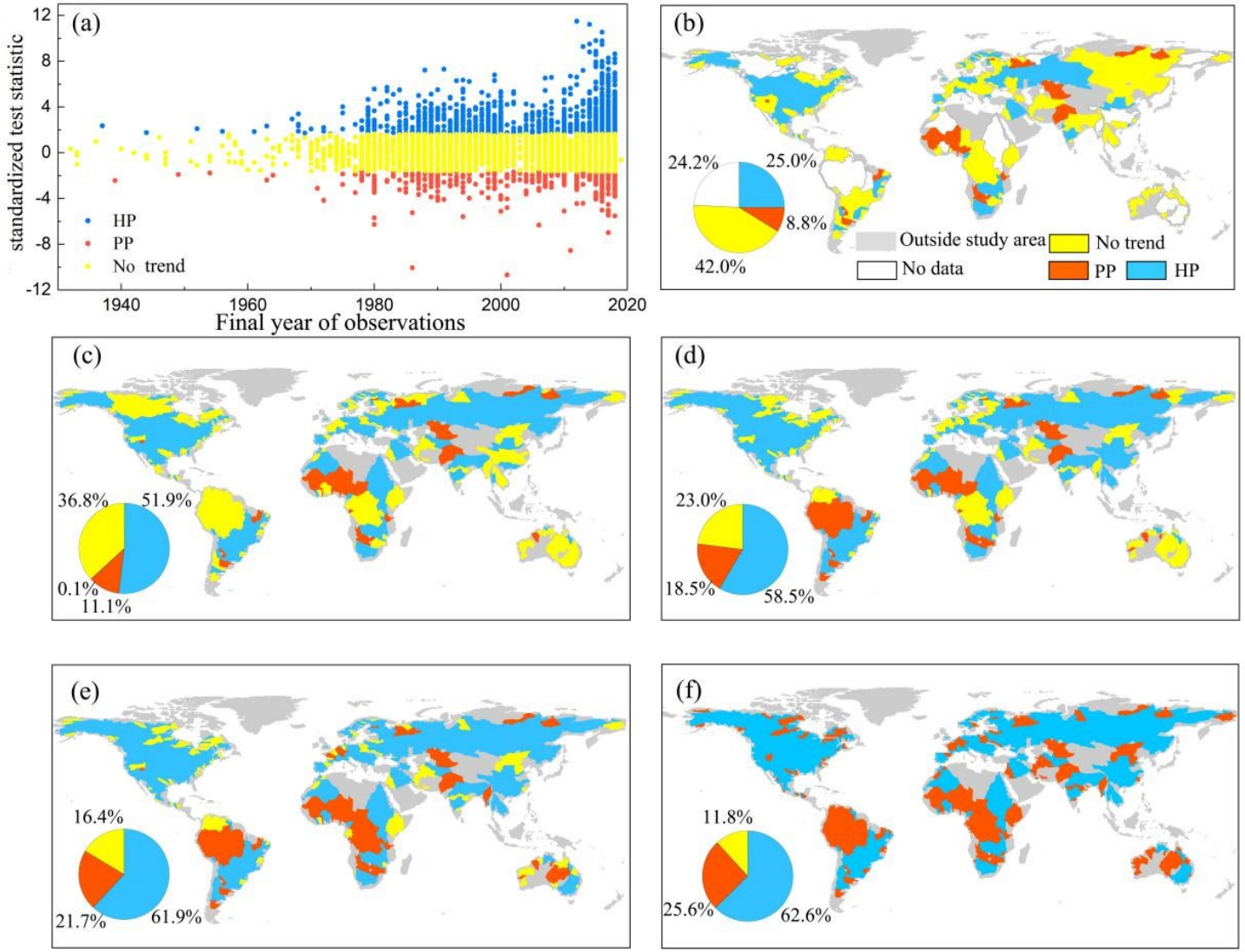

741

742 **Fig. 2.** Spatial-temporal variation characteristics of the water discharge homogenization (HP, in blue) and polarization (PP, in red) for 314 indepedent river
743 basins covering 66.1% of the Earth's land surface (8809.2×10^4 km^2). Panel (a) displays the variation trend in normalized water discharge at 5668 hydrological
744 stations during the dry season (checked using TFPM-MK trend test method). The remaining panels comprise distribution maps of HP and PP based on data

series extending to the period before 1980 (b), by the 1980s (c), by the 1990s (d), by the 2000s (e) and by the 2010s (f). Inset pie charts in (a), (b), (c), (d), (e) and (f) present the areal percentages of HP (in blue), PP (in red), and no phenomenon (in yellow) in the five periods.

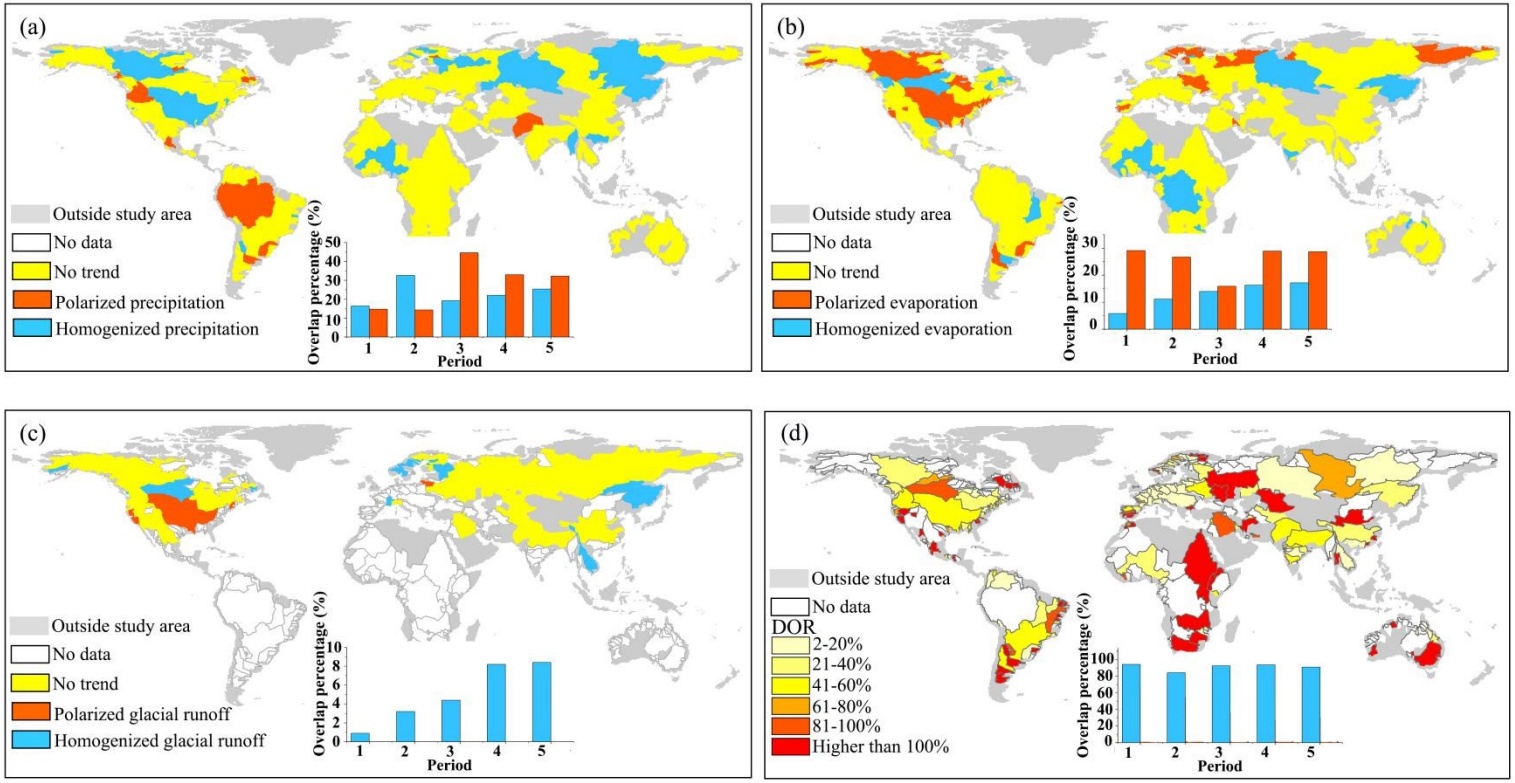

Fig. 3. Panels (a), (b) and (c) are distribution maps showing the homogenized and polarized precipitation, evaporation, and glacial runoff (represented by the blue and red patches on the world map, respectively). Panel (d) maps the degree of regulation (DOR) index observed in the last year of the water discharge series record for each basin. The histogram insets in (a) and (c) present percentages of drainage areas showing identical trends in precipitation and glacial runoff to the trends in seasonal water discharge during the five periods of interest (Period 1: before 1980; Period 2: by 1980s; Period 3: by 1990s; Period 4: by 2000s; Period 5: by 2010s); the histogram inset in (b) presents percentages of drainage areas showing opposite trends in evaporation to the trends in seasonal water discharge during the five periods; the histogram inset in (d) presents percentages of drainage areas experiencing both homogenization water discharge and significant regulation by dams (DOR >2%) during the five periods; the blue bars represent regions with homogenization of water discharges; the red bars represent areas with polarization in water discharges.